Journal of Alloys and Compounds 853 (2021) 156900

Contents lists available at ScienceDirect

Journal of Alloys and Compounds

journal homepage: http://www.elsevier.com/locate/jalcom

Enhanced electrochemical glucose sensing performance of CuO:NiO mixed oxides thin film by plasma assisted nitrogen doping

Maghmood Palmer [a], Milua Masikini [a], Li-Wen Jiang [b], Jian-Jun Wang [b], Franscious Cummings [c], Jessica Chamier [d], Omowumi Inyang [a], Mahabubur Chowdhury [a, *]

[a] Department of Chemical Engineering, Cape Peninsula University of Technology, Bellvile, 7535, South Africa
[b] State Key Laboratory of Crystal Materials, Shandong University, Jinan, Shandong, 250100, PR China
[c] Electron Microscope Unit, University of the Western Cape, Bellvile, 7535, South Africa
[d] Hysa Catalysis, University of Cape Town, Rondeboshc, 7700, South Africa

ARTICLE INFO

Article history:
Received 13 July 2020
Received in revised form
24 August 2020
Accepted 25 August 2020
Available online 6 September 2020

Keywords:
Nitrogen doping
Glucose detection
Plasma etching
Binder less deposition
CuO
Cu_2O
Phase transformation

ABSTRACT

In this study plasma-assisted nitrogen doping of a CuO−NiO mixed oxide thin film was presented. The as prepared film was also applied as a glucose sensor. The nitrogen species generated during plasma ignition resulted in a beneficial phase transformation of CuO to Cu_2O. Characterisation techniques such as XRD, SEM, EIS and Hall Effect etc. measurements were utilized to study the morphology, structural features, doping profile and electrical properties of the sensing material. Device performance electrochemical testing showed that the as-developed sensor (labelled as N−CuO/Cu_2O:NiO) showed an ultra-fast response time of 2.5 s with high sensitivity (1131 μA/mM.cm^2). The linear range of the sensor was calculated to be up to 2.74 mM of glucose and excellent selectivity towards glucose at an applied potential of +0.67 V vs Ag/AgCl in 0.1 M NaOH electrolyte solution. The limit of detection was calculated to be 20 μM for the N−CuO/Cu_2O:NiO sensor. The N−CuO/Cu_2O:NiO have smaller Tafel slope compared to pristine CuO and CuO:NiO mixed oxides. Enhanced electrochemical performance of the N−CuO/Cu_2O:-NiO originates from the improved electronic properties of the thin film.

1. Introduction

The cells in our body require energy to function, develop and reproduce [1,2]. Glucose is the most predominant carbohydrate used to source energy for human beings [3]. Diabetes Mellitus is described as a metabolic disease affecting the body's ability to secrete or use insulin effectively [4], resulting in uncontrollable blood glucose concentrations in the body. Persons afflicted with the disease is required to monitor and manage the disease [2] which can be stressful and costly. Currently, enzymatic glucose sensors are used to monitor blood glucose levels [5]. The perpetual advancement of technology has provided infrastructure able to produce the enzymatic strips effectively at incredible speeds by using of printing devices [6]. However, these rapidly produced sensors with proteins are vulnerable to proteases, which degrade and digest proteins on exposure [2]. Furthermore, numerous environmental conditions tend to shorten the life span of the enzymatic biosensor [2,7]. The disadvantages of enzymatic sensors have been addressed by developing non-enzymatic sensors with the ability to electrochemically react directly with glucose [2]. Xiao and co-authors (2019) state that the catalytic material plays a key role in glucose oxidation performance. Hence, choosing the right material for non-enzymatic glucose sensing is of extreme importance.

Transition metal oxides, such as NiO_x, FeOOH, MnO_2, RuO_2, CuO_x, ZnO and Co_3O_4 [8], have showed increased application potential as a result of relatively low costs, superior glucose sensing ability and avoids poisoning of the catalytic surface [9,10]. These metal oxides would oxidise glucose at constant potential creating a simplified process for detection [11]. Cu and Ni possesses good catalytic properties, are found in natural abundance, has good stability and is relatively cost effective [2,11]. Studies conducted by Espro and co-authors (2014) showed that the oxide form of copper has superior electro-catalytic properties compared to the pristine copper. Copper oxide is also a desirable material due to the

* Corresponding author.
E-mail address: chowdhurym@cput.ac.za (M. Chowdhury).

https://doi.org/10.1016/j.jallcom.2020.156900
0925-8388/

multivalent states which improve recovery of electro-catalyst [2]. Redox activation of the electrode material plays an important role in enhancing sensitivity of electrode materials for non-enzymatic glucose sensing. Lu and co-workers demonstrated that presence of multiple oxidation states in CuO/Cu_2O composite material improved the electrochemical performance of the material compared to its pristine counterpart [12]. In an earlier work Nitrogen doping of CuO thin film at low temperature annealing condition has been shown to partially convert CuO to Cu_2O within the film. The incorporation of nitrogen atoms significantly reduces the resistivity of the thin film [13]. Previously, NiO, a p-type semiconductor has been utilized as a dopant to enhance the electrochemical properties of the CuO microfibres [15]. Therefore, it is only rational, to design a CuO/Cu_2O:NiO composite material and evaluate the developed material for nonenzymatic glucose detection.

Traditionally developing an electrode for sensing applications is a twostep process. Firstly, the nanomaterials are prepared via various synthesis routes, such as hydrothermal, solvothermal, and solgel etc. Finally, the prepared nanostructured materials are drop casted on a conductive substrate with a binder. The presence of binder introduces contact resistance which ultimately can reduce electrical conductivity of the materials [16]. Moreover, the adhesion of the materials on the substrate is always an issue. Direct growth of nanostructured materials via hydrothermal technique is being used recently. However, controlling the film thickness and film homogeneity is challenging in this method. Techniques such as, plasma sputtering and atomic layer deposition can deposit uniform controlled film on a substrate however the use of ultrahigh vacuum makes these processes capital intensive. Solution deposition techniques can be used to develop low cost electrode with controlled film thickness. In our previous work [16–18] we have used a solution based technique to deposit Co_3O_4 thin film. However, one of the biggest drawback of the developed method is the lack of phase and morphology control of the deposited film. Hence, It is our interest in this work to deposit a) CuO:NiO thin film and b) induce phase transformation of CuO to Cu_2O within the deposited CuO:NiO thin film by plasma assisted nitrogen doping. It was rationally designed to utilise the mixed oxidation sate of CuO/Cu_2O together with the NiO doping for enhanced electrochemical activity towards glucose oxidation. The as developed plasma assisted nitrogen doped mixed oxide (N–CuO/Cu_2O:NiO) thin film showed excellent glucose sensing ability with very high selectivity and ultrafast response time. Various physical and electrochemical characterisation techniques were used and discussed to probe the origin of the enhanced electrochemical activity in the following sections.

2. Experimental methods

2.1. Materials

Copper (II) chloride dihydrate ($CuCl_2.2H_2O$), nickel (II) nitrate hexahydrate ($Ni(NO_3)_2.6H_2O$), d-(+)-glucose, ascorbic acid (AA), uric acid (UA), sucrose, fructose, human serum, sodium hydroxide (NaOH), sodium oleate ($C_{18}H_{33}NaO_2$) and fluorine doped tin oxide (FTO) glass were purchased from Sigma Aldrich South Africa and used without any further purification procedures.

2.2. Mixed oxide thin film electrode fabrication

Copper oleate was synthesised by ion exchange reaction between $CuCl_2.2H_2O$ and $C_{18}H_{33}NaO_2$ as reported in previous studies [20]. FTO glass slides were cut to size (1.2 × 4.5 cm) and extensively washed in an ultrasonic bath using detergent or degreaser for 10min, ethanol bath for 10min and finally in water for 10min as well. The FTO glass slides were dried in a 60 °C oven over night following the cleaning procedure. Solution A of 0.09 g copper oleate was dispersed, via ultrasonication, in 0.5 ml of toluene and solution B of 0.01 g $Ni(NO_3)_2.6H_2O$ was dispersed in 0.5 ml of ethanol. To vary the concentration of nickel within the precursor, to be spin coated, solutions A and B were mixed thoroughly via ultrasonication in various volumetric percentage ratios (70:30, 80:20, 90:10 and 95:5). A 50 μL of the precursor solution was deposited onto the cleaned FTO glass and spin coated in a twostep process to minimise edge/corner beads forming and thus creating a more uniform layer on the FTO glass [16]. The FTO glass with precursor was spun at 1000 rpm for 10s followed by 4000 rpm for 50s. Thereafter, the glass electrode was calcined at 350 °C for 10min creating a thin film of mixed oxide material. The deposition, spin coating and calcination were repeated for 1–6 times (each repetition is described as another layer forming onto the FTO glass slides) to achieve an optimum film thickness for improved electrochemical experiments.

2.3. Plasma assisted nitrogen doping of mixed oxide thin film

To obtain the nitrogen doping, the films were plasma irradiated in a custom-built plasma-enhanced chemical vapor deposition chamber at a base and treatment pressure of 1.5×10^{-6} and 7×10^{-2} mbar, respectively. Beforehand, the plasma power was fine-tuned in a N_2:Ar mixture by maintaining a constant gas flow rate of 100:100 sccm. An optimized plasma power of 500 W (plasma power supply = 5 V; 1.25 A) yield the most consistent and significant changes in performance of the films. Once set, the Ar flow was reduced to 0 sccm, which then yielded the red glowing N_2 plasma. This point also signalled the start of the treatment, which was set at 10 min for all samples. A summary of the electrode fabrication process is presented in Fig. 1.

2.4. Electrochemical experiment

The electrochemical experiments were all conducted using an Autolab PGSTAT302 N potentiostat (Metrohm, Switzerland). These experiments made use of a three-electrode setup: the as prepared electrodes as working electrodes, a reference electrode of Ag/AgCl and a counter electrode of platinum wire. A solution of 0.1 M NaOH was used as the electrolyte for both cyclic voltammetry and chronoamperometry experiments. The cyclic voltammetry experiments were recorded using a potential range from −0.1 V to 0.8 V vs Ag/AgCl at 25 mV/s. Constant stirring conditions were applied for the chronoamperometry experiments using an applied bias potential of +0.67 V vs Ag/AgCl. EIS experiments were conducted in a 0.1 M NaOH solution. A bias potential of 0.3 V was used with 10 mV amplitude as the applied AC voltage in a frequency range between 1-10^6 Hz and plotted to generate the complex plane diagrams (Nyquist plot).

2.5. Surface characterisation

The material phase was identified using X-ray diffraction (XRD). The prepared samples were characterized by a Bruker D8 ADVANCE with a Cu Kα radiation source (λ = 0.154178 nm) operated at a tube voltage of 40 kV and a current of 40 mA. The diffraction patterns were collected by step scanning in the 2θ range of 10–70° with an increment of 0.0216°. X-ray photoelectron spectroscopy (XPS) analysis was performed on a PHI X-tool fully automatic scanning microregion XPS probe (Ulvac-Phi) using monochromatic aluminum as the excitation source. The survey spectra were recorded with a pass energy of 160 eV and high-resolution spectra with a pass energy of 40 eV. Zeiss Auriga field emission scanning electron microscope was used to study the morphology of the films

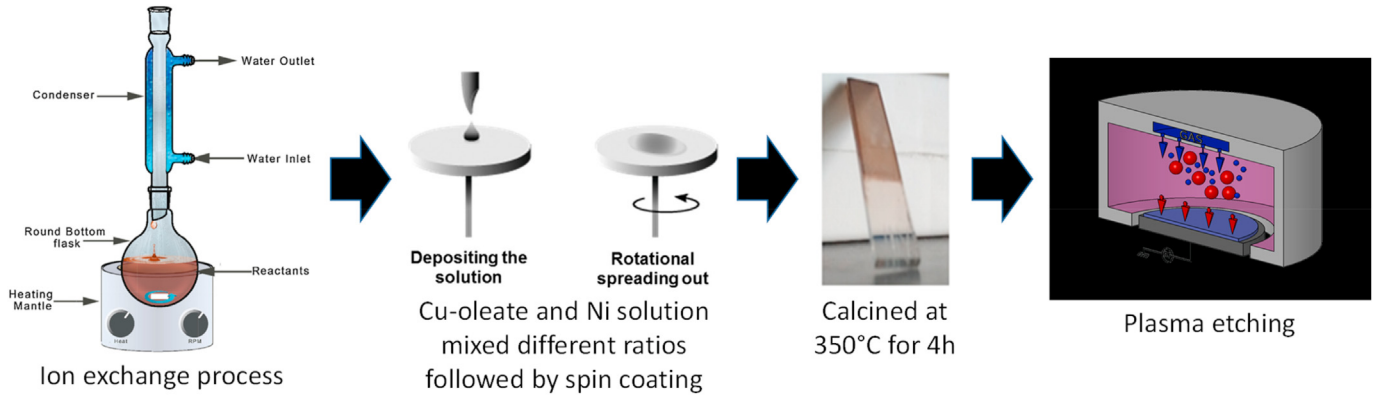

Fig. 1. Schematic of electrode fabrication process.

produced. All thin films were imaged using an in-lens secondary electron detector with the beam accelerated to an electron high tension of 5 kV. Energy dispersive x-ray spectroscopy was used to quantify the elemental composition of the films; an Oxford X-max solid-state drift detector was used in this regard, with the electrons accelerated to 20 kV. The electrical transport properties of the films were investigated with Hall Effect measurements using an Ecopia HMS-3000 Hall Effect Measurement System with a 0.55 T (T) permanent magnet operated at room temperature. Input currents ranging from 100 to 1000 μA, with 6 measurements on different areas per input current, were applied to reduce the systematic errors and obtain a narrow distribution in mobility, carrier density, resistivity, and dopant concentration.

3. Results and discussion

3.1. Surface characterisation of the thin film electrode

X-ray diffraction is a tool that can identify the structural features of various chemical compounds and nanoparticles [21]. The analysis of Fig. 2a suggests that a base-centred monoclinic structure of CuO is present in the pristine film [22,23]. The diffraction patterns were observed to be at 2θ = around 35.56°; 37.74°; 38.76°; 54.50°; and 61.61° corresponding to (002), (111), (200), (−020), and (−113)

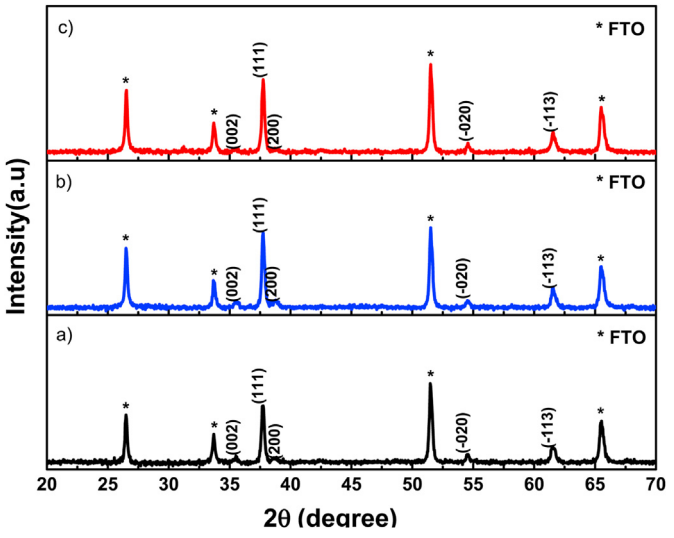

Fig. 2. XRD diffractogram of the a) Pristine CuO film, b) Plasma treated CuO film and c) film prepared with Nickel precursor.

respectively, in accordance with the JCPDS Ref. 045−9537 and JCPDS Ref.80−0076 [22]. This result confirms the presence of CuO. The addition of Nitrogen via plasma etching has no clear effect on the diffractogram obtained as seen in Fig. 2b. The diffractogram shows the peaks of CuO in the nitrogen doped CuO film without showing any significant shifts or broadening of XRD peaks of pristine CuO. No Cu_2O peaks were observed in XRD patterns. However, it does decrease the intensity of the peaks similar to previously published report [24,25]. It is observed from Fig. 2c that the introduction of nickel precursor in the copper oleate precursor during the synthesis decreased the XRD peak intensity of the resulting film. However, Fig. 2c suggests that no conclusive Ni or NiO peaks are observed in the diffractogram. The absence NiO or Cu_2O characteristic peak might suggests that the quantity of NiO or Cu_2O present is below the detection limit of XRD techniques employed. No additional peaks or changes were observed in XRD pattern after plasma treatment of the aforementioned film (data not shown).

XPS data of the pristine CuO electrode (Data in Brief Fig. 1) shows a $Cu2p_{3/2}$ peak at 933.3 eV followed by the two satellite peaks at 940.9 and 943.4 eV. Moreover, it also shows a $Cu2p_{1/2}$ peak at 953.3 eV and its satellite peak at 961.8 eV which matches the standard CuO XPS spectrum [26,27]. The oxygen binding energy of peaks 529.3 eV, which represents a common (metal) M − O bond [28,29], and 531.0 eV confirms the existence of oxygen in the CuO lattice and hydroxyl absorption which takes place on the electrode surface [27,30]. The O1s peak observed at 531.8 eV suggest that carbon contaminants are present on the electrode material, which indicates a C═O bond [31]. This is as a result of the sensor being stored in air. These results confirm the presence of CuO in the pristine electrode and agrees very well with the results obtained from the XRD analysis.

Introducing nitrogen into the pristine CuO electrode by plasma treatment suggests the presence of Cu(I) due to the $Cu2p_{3/2}$ peak observed at 932.5 eV and $Cu2p_{1/2}$ peak at 952.7 eV [13,32]. The XPS data (Data in Brief Fig. 2) also shows a peak observed at 934.3 eV, indicating the presence of $Cu(OH)_2$ [33]. The N1s spectrogram shows a clear presence of nitrogen within the plasma treated CuO electrode with a peak observed at 397.2 eV. This N1s peak indicated the existence of a M − N species in the form of pyridinic nitrogen [34,36,37]. A N1s peak of 398.5 eV hints to the existence of C−N [34] which may be a result of contamination with common hydrocarbons in the air. Literature suggests that a N1s peak of 403.4 eV creates a nitrite bond of $N-O_2$ with the host structure [38,39] and the binding energy of 406.8 eV suggest that other oxidised nitrogen species are present [40].

A Ni $2p_{3/2}$ peak of 855.5 eV was observed (Fig. 3) for the as prepared electrode corresponding with a satellite peak at 861.2 eV

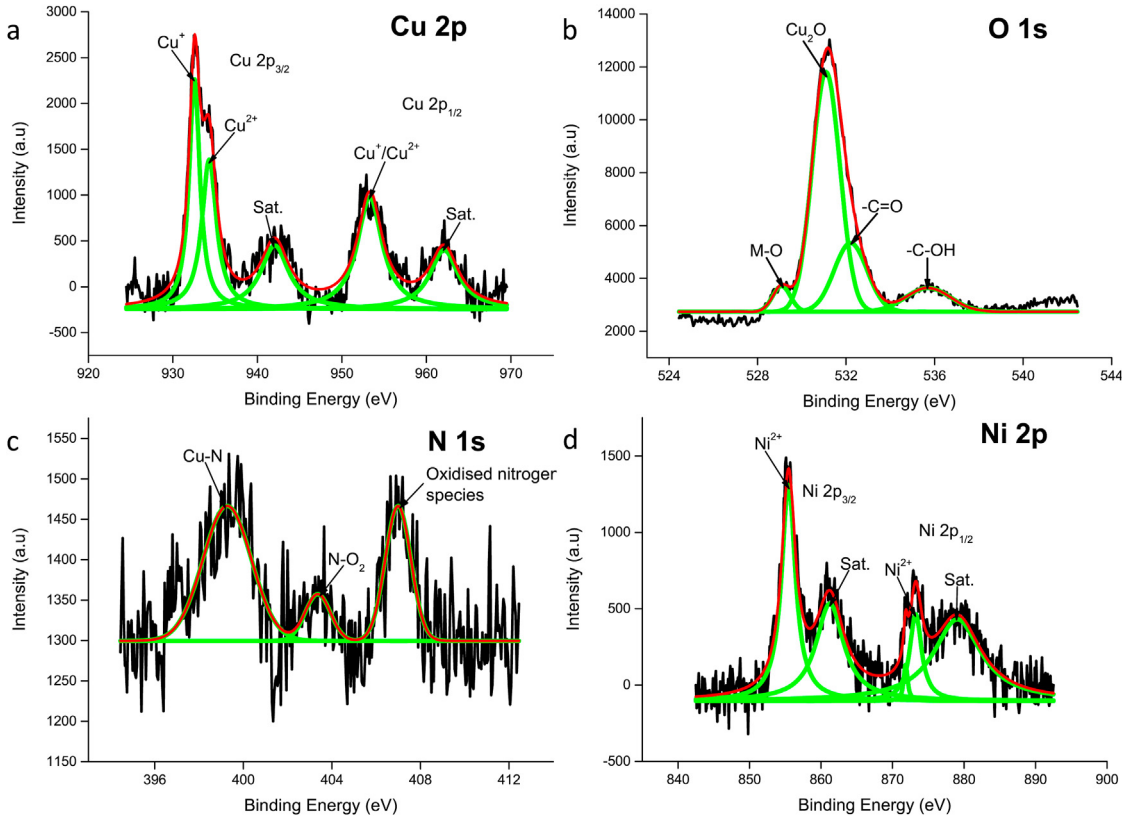

Fig. 3. XPS spectrogram of the plasma treated CuO:NiO film developed sensor.

suggesting that this thin film electrode has NiO within the active material [2,37]. Simultaneously, a Ni $2p_{1/2}$ peak at 873.2 eV and a satellite peak at 880.1 eV further confirm the existence of NiO. The slight increase in binding energy of Ni compared to the standard suggests that there are interactions with other species [41]. The corresponding Cu spectrum also shows the presence Cu_2O, however, the presence of Ni increases the binding energy suggesting interactions between Cu and Ni in the as prepared electrode. The binding energy of the O1s spectrum at 529.1 eV also confirms the existence of NiO [2,37] and 532.1 eV correspond to the formation of Cu_2O [2,32] within the as prepared electrode. Nitrogen incorporation enhances the electrical conductivity as a result of the availability of p-electrons [37]. However, interactions of the metals with this element is present due to the lower binding energies of Cu [41]. Moreover, the presence of Cu $2p_{3/2}$ peaks of 932.5 and 934.4 eV suggest the presence of $Cu(OH)_2$ together with Cu_2O in the electrode [10,32]. The N1s spectrum suggest that pyrrolic nitrogen is present due to the peak of 399.3 eV, which corresponds to a M − N bond [37]. The other peaks are consistent with the N1s spectrum observed for the plasma treated CuO electrode. Therefore, it is clear that phase conversion of CuO to Cu_2O occurs during plasma assisted nitrogen doping. Hence the as prepared electrode labelled as N−CuO/Cu_2O:NiO will be discussed from here unless otherwise stated. XPS data of the N−CuO/Cu_2O:NiO after electrochemical testing showed no changes in the spectrogram compared to virgin electrode (Data in Brief Fig. 3). This highlights the chemical stability of the N−CuO/Cu_2O:NiO electrode.

Morphology of the thin film electrodes were analysed by scanning electron microscopy (SEM). The SEM images (Fig. 4a) of the pristine CuO electrode shows a crack free layer with a slight roughness across the surface. Post plasma treatment however, it is observed that the surface roughness became much smoother and more consistent (Fig. 4b). This suggests that the introduction of nitrogen via plasma treatment etches the surface roughness of the pristine CuO electrode [42]. Plasma etching with nitrogen had no destructive effects observed on the film morphology. Introducing the nickel precursor into the pristine CuO, as can be seen in Fig. 4c, creates cube-like structures of NiO (as was confirmed by XPS characterisation) forming on top of the base layer of active material. Plasma treated (Fig. 4d) CuO/NiO electrode shows that the clusters become more pronounced and the average particle size distribution is more centralised at 200−400 nm (Data in Brief Fig. 4). The presence of Ni and N was also observed from the energy dispersive X-ray spectroscopy, EDX as shown in Fig. 4e cementing the conclusion obtained from XPS data.

The carrier concentration and mobility of free electrons within an electroactive material can be determined using the Hall Effect technique [43–45]. Literature suggest that higher mobility is preferred as it results in a lower carrier concentration which produces less optical reflection and absorption [44]. The N−CuO/Cu_2O:NiO electrode demonstrates *N*-type semiconducting nature as a result of the negative bulk concentrations [45]. The free electron mobility and conductivity of the N−CuO/Cu_2O:NiO electrode is found to be 34.43 cm^2/V and 3187 1/Ωcm respectively. This is higher than the pristine CuO thin film (29.27 cm^2/V and 3030 1/Ωcm for free electron mobility and conductivity respectively). The improved mobility of this electrode is due to an improved crystallinity and limited scattered centres for the charge carriers of the developed sensor [45].

3.2. Electrochemical behaviour of the N−CuO/Cu_2O:NiO thin film electrode

The electrochemical performance of the developed sensors towards oxidation of glucose is evaluated using cyclic voltammetry (CV). CV experiments were conducted in alkaline solution of 0.1 M

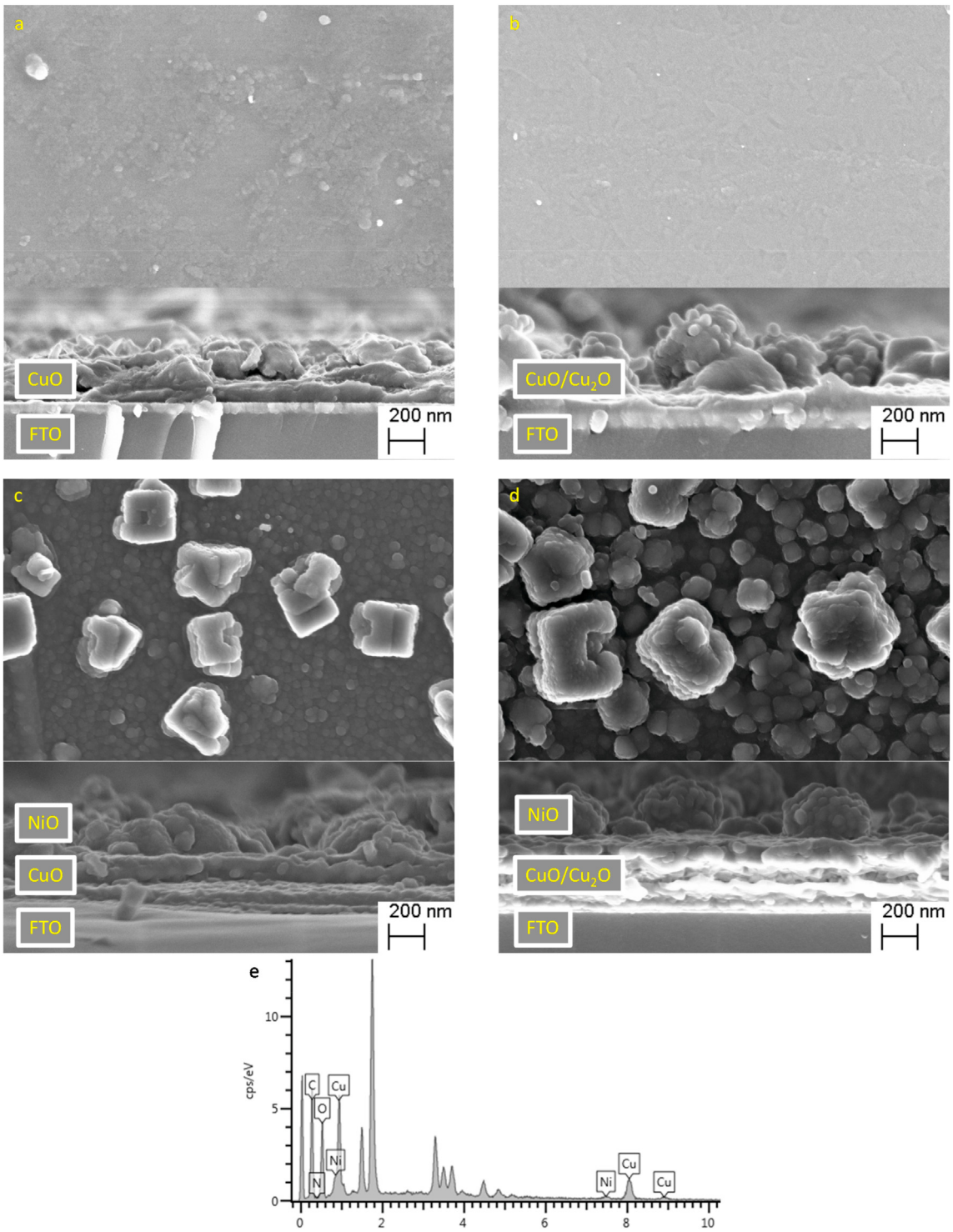

Fig. 4. SEM images of top and cross-sectional area of a) CuO, b) N–CuO/Cu_2O, c) CuO:NiO, d) N–CuO/Cu_2O:NiO sensors and e) EDS spectrum of the N–CuO/Cu_2O:NiO sensor.

NaOH using a potential range from −0.1 V to 0.8 V vs Ag/AgCl at a scan rate of 25 mV/s [28,46]. An alkaline solution of NaOH is used since carbohydrates such as glucose can be oxidised at high pH [47]. Experiments conducted by Zhang and Coauthors (2014) [46] suggest that an increase in concentration of NaOH solution relates to an increase in peak current during glucose oxidation, due to the increased availability of hydroxyl radicals (OH^-) which are used in the glucose oxidation mechanism. Furthermore, the concentrations of 0.05 M and 0.1 M NaOH has limited increase in oxidation peak current [46]. However, a 0.1 M NaOH is used due to the excess availability of OH^- ions [2,15,46].

Electrodes prepared using the ratio of 70:30 (%V/V) copper to nickel precursor demonstrated the best electrochemical activity compared to the other ratios studied (Data in Brief Figure 5a). However, any increase above 30% Ni content decreased the electrochemical performance of the electrode (Data not shown). Effect

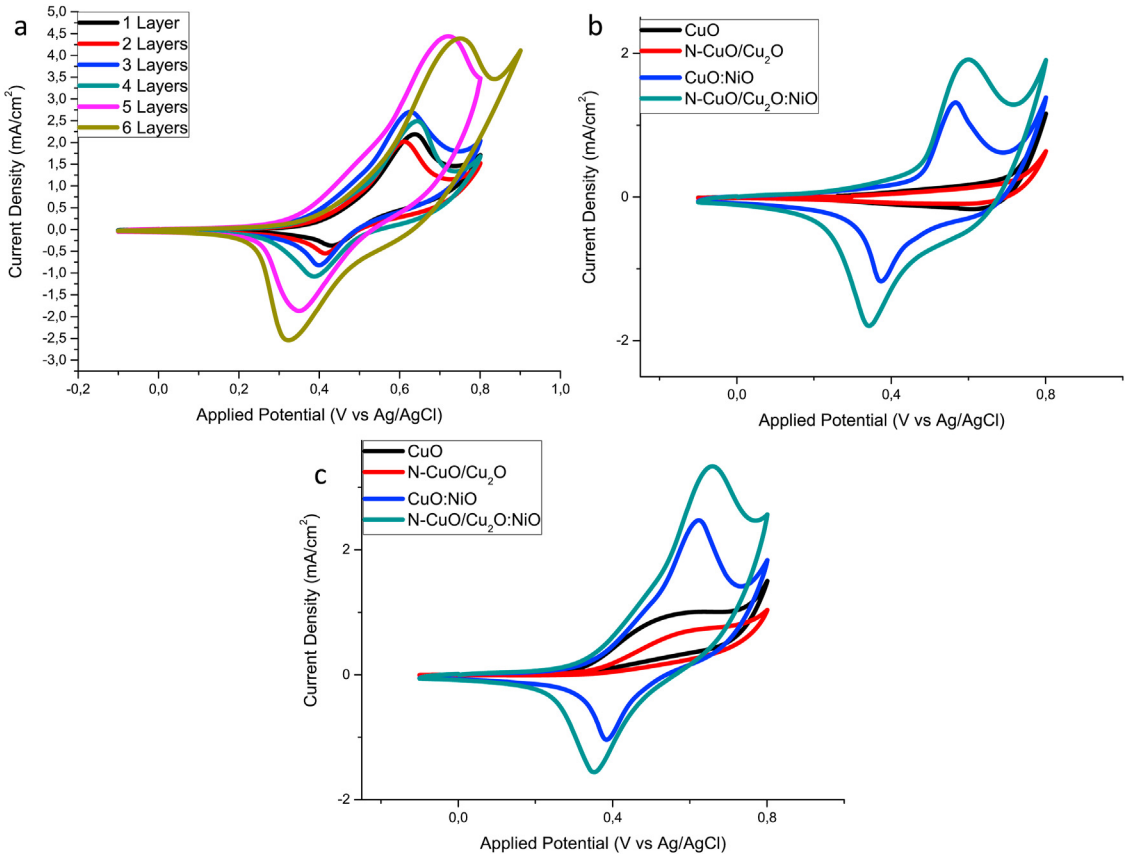

Fig. 5. CV diagrams at 25 mV/s of a) various layers of the N–CuO/Cu_2O:NiO sensor, b) comparison of the different developed sensors in 0.1 M NaOH and c) comparison of the different developed sensors in 1 mM glucose.

of film thickness (number of layer) on the electrochemical performance of the N–CuO/Cu_2O:NiO electrode prepared with 70:30 (%V/V) precursors was investigated by cyclic voltammetry (Fig. 5a) in the presence of 1 mM glucose. The result shows that with increasing film thickness the current response of the electrodes increases up to layer no 5. With further addition of layer, no significant increase in the oxidation current was observed. Hence, only 5 layer deposited N–CuO/Cu_2O:NiO electrodes were further evaluated. All data reported from this point onward is for the aforementioned electrodes unless otherwise stated.

The electrochemical performance of Pristine CuO, N–CuO/Cu_2O, CuO:NiO and N–CuO/Cu_2O:NiO, was probed using cyclic voltammetry (CV) in both the absence and presence of 1 mM glucose in 0.1 M NaOH electrolyte solution at scan rate of 25 mV/s. Cyclic voltammograms are shown in Fig. 5b and c. As can be seen in absence of glucose (Fig. 5b), in the cases of CuO and N–CuO/Cu_2O electrode no oxidation peak has been observed but a large oxidative tail is observed for both electrodes due to the onset of water splitting thus overshadowing peak associated to CuO/CuOOH transition. In Contrast the CuO:NiO and N–CuO/Cu_2O:NiO electrodes (Fig. 5b), shows an oxidation peak at 0.56 mV and 0.60 mV for CuO:NiO and N–CuO/Cu_2O:NiO, respectively. In the reverse scan (Fig. 5b), the CV shows a reduction peak and a broad peak for both electrodes. The cathodic peak at 0.37 mV and 0.34 mV represent the active dissolution of nickel (or NiOOH/NiO transition) [48] and broad cathodic peak at 0.617 mV and 0.60 mV assigned to CuOOH/CuO transition for CuO–NiO and N–CuO/Cu_2O:NiO, respectively. Compared with CuO and N–CuO/Cu_2O, the CuO:NiO and N–CuO/Cu_2O:NiO showed higher oxidation peak currents (oxidation and reduction peak) with N–CuO/Cu_2O:NiO electrode being the highest and a small decrease in the values of peak potential. So, it is confirmed that the plasma assisted nitrogen doping and presence of NiO significantly increases the electrochemical activity.

In the presence of 1 mM glucose, the four developed electrodes i.e. CuO, N–CuO/Cu_2O, CuO:NiO and N–CuO/Cu_2O:NiO were able to oxidise glucose (Fig. 5c). Thus, an and enhancement in peak current were observed in all cases. The pristine CuO electrode oxidises glucose at around 0.55 V, The following irreversible reactions show the electrocatalytic oxidation of glucose mechanism taking place on the CuO sensor [26,28]:

$$CuO + OH^- \rightarrow CuOOH + e^- \quad (1)$$

$$2CuOOH + glucose \rightarrow 2CuO + gluconolactone + H_2O \quad (2)$$

Doping the CuO electrode with nitrogen negatively affected the oxidation peak as seen in Fig. 5b and c. This can be attributed to the fact that the plasma treatment alone decreases surface roughness as was seen in the SEM images. From the results observed during XPS analysis, a predominant Cu_2O peak was present in the plasma treated CuO sensor, which has a direct effect on the oxidising ability of glucose. Literature suggests that CuO has improved electro-oxidation capabilities compared to Cu_2O [49] which explains the lower glucose oxidation peak for N–CuO/Cu_2O compare to CuO as seen in Fig. 5b and c. The mechanism used for the oxidation of glucose using mixed copper oxide can be described by the following equations [49]:

$$Cu_2O + 2OH^- + H_2O \rightarrow 2Cu(OH)_2 + 2e^- \quad (3)$$

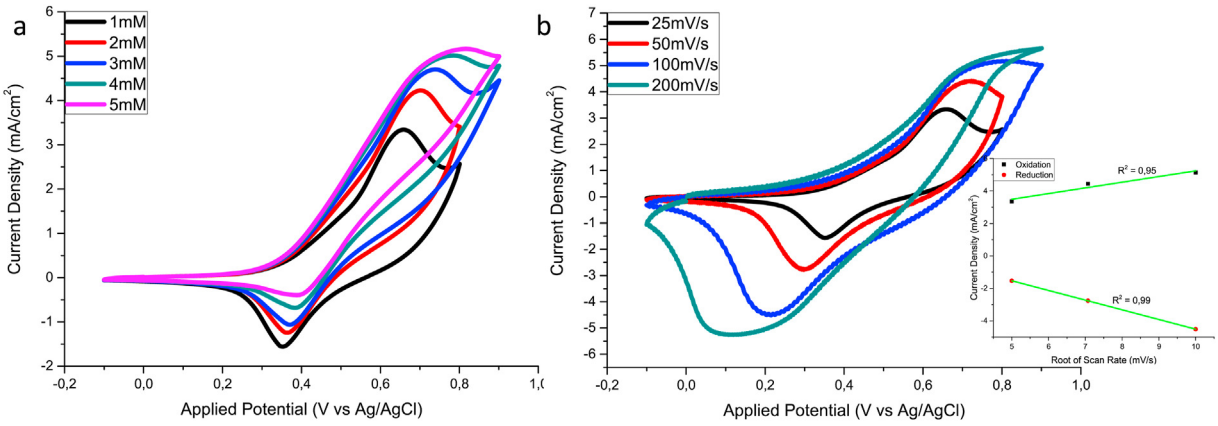

Fig. 6. CV diagrams of the N–CuO/Cu_2O:NiO sensor with a) various concentrations of glucose at 25 mV/s and b) various scan rates with inset of linear relationship between square root of scan rate and peak current density.

$$Cu(OH)_2 + OH^- \rightarrow CuOOH + H_2O + e^- \quad (4)$$

$$CuO + OH^- \rightarrow CuOOH + e^- \quad (5)$$

$$CuOOH + glucose \rightarrow Cu(OH)_2 + gluconolactone \quad (6)$$

Literature suggests that Cu^{3+} species act as the mediator for electron transferability during glucose oxidation, which require the presence of oxide, hydroxide and oxyhydroxide groups within an alkaline medium [49]. Thus, the N–CuO/Cu_2O electrode would create gluconolactone through the catalysation of glucose, as seen in equations (3)–(6), due to the peak observed at approximately 0.6 V [49]. The glucose oxidation peak current for CuO:NiO electrode is significantly higher compared to pristine CuO and N–CuO/Cu_2O electrodes. However, the oxidation occurs at a slightly higher positive potential compared to the CuO and N–CuO/Cu_2O electrodes. The NiO species can also be involved in the oxidation reaction with glucose which creates a redox reaction as follows [37,50]:

$$NiO + OH^- \rightarrow NiOOH + e^- \quad (7)$$

$$NiOOH + glucose \rightarrow Ni(OH)_2 + e^- + gluconolactone \quad (8)$$

The CuO:NiO electrode uses equations (5)–(8) during the electrooxidation of glucose which can be deduced by the peak observed at 0.62 V [26]. Moreover, the presence of the NiO creates a multi-species composition which has a synergetic effect on the promotion of glucose oxidation [17,26,28]. Nitrogen doping the CuO:NiO film further improved the electroactivity of the electrode as observed in Fig. 5b and c and the mechanism for the catalysation of glucose into gluconolactone is observed through equations (3)–(8). This mechanism for the electrooxidation of glucose is used as a result of the peak observed at 0.67 V, which is greater than the experiments conducted by Ref. [26]. According to literature, the presence of nitrogen increases the applied potential required for the oxidation of glucose compared to the electrode without nitrogen [51,52]. The improved electrocatalytic ability of the N–CuO/Cu_2O:NiO electrode may be the result of the availability of greater catalytic active sites and a pair of electrons for conjugation, provided by the nitrogen's π-conjugated rings, introducing electron donor characteristics for the electrode [52]. Furthermore, this improved electroactivity is due to the enhanced electron transfer ability due to increase in electronic conductivity as was confirmed by the Hall effect measurement in earlier section [51,53]. The glucose sensing ability of the N–CuO/Cu_2O:NiO electrode were evaluated by increasing glucose concentration from 1 mM to 5 mM (Fig. 6a). It can be clearly seen that the oxidation peak current increases significantly with increasing glucose concentration. At glucose concentration of 5 mM, the response of the sensor to glucose has started to reach saturation. For better investigation of the electrochemical behavior of the N–CuO/Cu_2O:NiO sensor cyclic voltammetry studies were performed in a 0.1 M NaOH solution containing 1 mM glucose at various scan rates. The anodic and cathodic peaks current increase with an increase in scan rate applied, as shown in Fig. 6b. In addition, the reduction potential shifts negatively and the oxidation potential shifts positively with the increase of scan rate. The good linear relationship between the square root of the scan rate and the redox peak current would indicate a diffusion driven process which is a relatively fast [14,16,26] and reversible electron transfer reaction [55,56]. This linear relationship can be observed in the inset of Fig. 6b until 100 mV/s. However, at higher scan rates (200 mV/s) the reaction becomes too slow and equilibrium cannot be reached timeously, as the current takes longer to respond to the applied potential creating an irreversible electron transfer reaction [55,56].

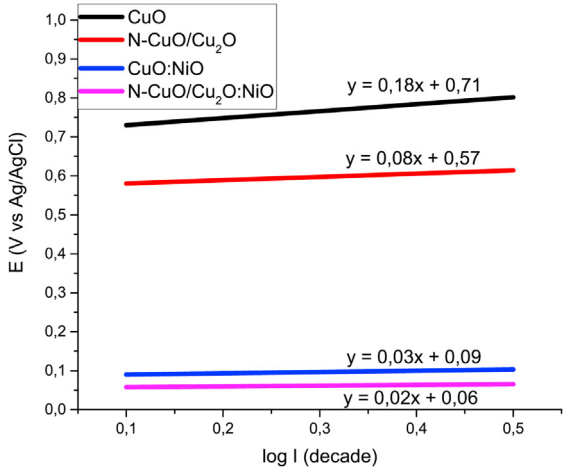

Fig. 7. Tafel slope diagram of the various developed electrodes.

To further understand the enhanced electrochemical performance of the N–CuO/Cu_2O:NiO electrode Tafel slopes of the different developed electrodes were obtained in 0.1 M NaOH solution containing 1 mM glucose as shown in Fig. 7. The Tafel slopes followed a trend as CuO > N–CuO/Cu_2O > CuO:NiO > N–CuO/

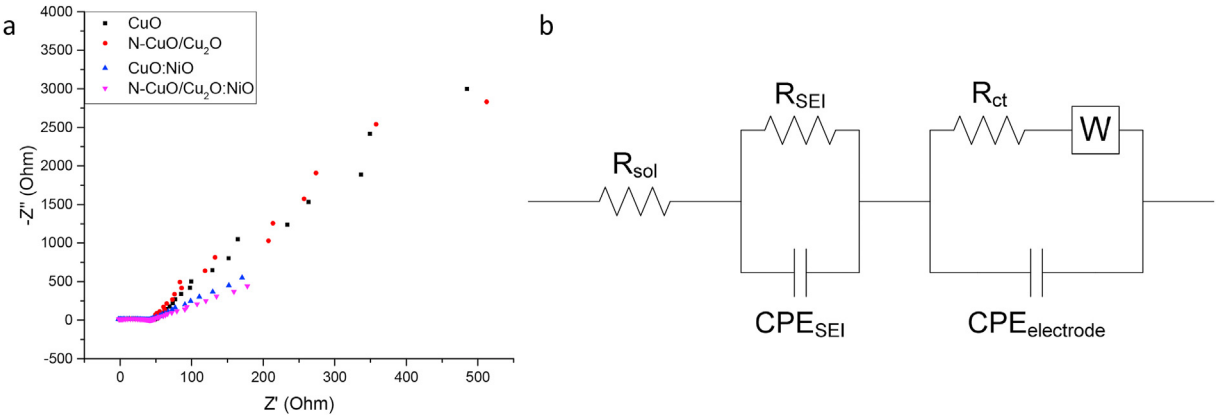

Fig. 8. a) Nyquist plots of the CuO and N−CuO/Cu_2O:NiO sensors and b) Schematic of the equivalent circuit used for fitting.

Cu_2O:NiO. The lowest Tafel slope value of the N−CuO/Cu_2O:NiO electrode highlights that the plasma assisted nitrogen doping and presence of NiO enhances the charge transferability of the material [24,57].

Electrochemical impedance spectroscopy was used in this study to investigate the electrochemical characteristic of N−CuO/Cu_2O:NiO electrode. The Nyquist plot of the developed sensors obtained is shown in Fig. 8a and the fitted equivalent electrical circuit can be observed in the Data in Brief Fig. 6. The Nyquist plots exhibit two depressed semi-circles and a straight line in the low-frequency region. The semi-circle represented at higher frequencies region can be assigned to the double layered capacitance of the electrode-electrolyte interaction and the overall charge transfer resistance (R_{ct}) [35,58], the semi-circle at lower frequencies can be assigned to the faradaic reaction [59], and the linear diffusion can be modelled using a Warburg impedance (W). Constant phase elements (CPE) are used instead of a regular capacitor to achieve a more accurate modelling of the EIS data [60]. An equivalent electrical circuit proposed for fitting the data, related to the various developed sensors in 0.1 M NaOH, is shown in Fig. 8b. This is an approximation of the complex plane system generated by the EIS experiments [35,60]. The circuit at the limit of high frequency quantifies the solution resistance (R_{sol}) representing the flow of electrons through the electrolyte solution [35,59]. The elements represented by R_{SEI} and CPE_{SEI} models the solid electrolyte interface (SEI) diffusion impedance [35,58]. The charge transfer resistance (R_{ct}) quantifies the resistance to the flow of ions at the electrode and electrolyte interface [58]. The R_{ct} values achieved from the modelled equivalent electrical circuit are presented in Table 1. The results suggest that the CuO:NiO electrode has the best R_{ct} value compared to the other electrodes. However, the N−CuO/Cu_2O:NiO exhibits a smaller R_{ct} value compared to the CuO and N−CuO/Cu_2O electrodes. This results coupled with Hall effect and Tafel plot measurements discussed earlier demonstrates the enhance electrochemical performance of the N−CuO/Cu_2O:NiO electrode.

Table 1
Charge transfer resistance calculated for each developed sensor.

Material	R_{ct} (Ω)	Estimated Error (%)
CuO	60.53	2.89
N−CuO/Cu_2O	56.75	3.11
CuO:NiO	53.20	2.71
N−CuO/Cu_2O:NiO	54.18	2.75

3.3. Chronoamperometric study of the N−CuO/Cu_2O:NiO electrode

Various concentration of glucose was added successively at an interval of 30s (Fig. 9a) under stirring at a potential of 0.67 V in a solution of 0.1 M NaOH to evaluate the sensor performance via chronoamperometric study [14,17]. A typical step response [54] is observed with a rapid response time of 2.5s towards successive additions of glucose. The dose response curve is presented in Fig. 9b and can be quantified using the equation Current (I) = 1.131X + 0.234 for the linear range of 0.05−2.74 mM of glucose with a sensitivity of 1131 μA/mM.cm^2. The detection limit of the sensor was calculated to be 21 μM at S/N = 3. A comparison of the performance characteristics is observed in Table 2 for all the developed sensors, which highlights the superiority in glucose sensing ability of the N−CuO/Cu_2O:NiO compared to the other developed sensors. The corresponding amperometric responses for the CuO, N−CuO/Cu_2O and CuO:NiO sensors is presented in Data in Brief Figs. 7−9 respectively.

3.4. Selectivity, repeatability and shelf life

Selectivity, repeatability and shelf life are important characteristics for practical application of the developed sensors [17,28,51]. The selectivity of the electrode was performed in the presence of interference species i.e. uric acid, ascorbic acid, sucrose, and fructose (Fig. 9c). Literature suggest that in physiological fluid i.e. blood, glucose concentrations are 10 times greater than the interference species mentioned above [61,62]. Therefore, 200 μM of glucose was used during the selectivity tests compared to 20 μM of the interference species using the same applied potential as used for the chronoamperometric experiments [16,17]. The N−CuO/Cu_2O:NiO developed sensor are selective towards glucose at the specified potential showing minimal interference with other species. The N−CuO/Cu_2O:NiO sensor still showed a response to glucose after the successive additions of interference species (Fig. 9c). This highlights that the surface of the electrode is not poisoned by the presence of the interference species. A comparison of the as prepared sensor with commercial glucose meter produced comparative results (RSD of 5%). These findings demonstrate the potential of the as prepared electrode as a glucose sensor.

During the repeatability tests, the electrode is rinsed with deionized water and air dried using a compressed air blower, removing excess moisture and impurities, after testing one CV cycle. This procedure was repeated for five CV cycles and the results obtained were calculated accordingly. Similarly, the electrodes were washed and dried after a CV cycle for the stability testing,

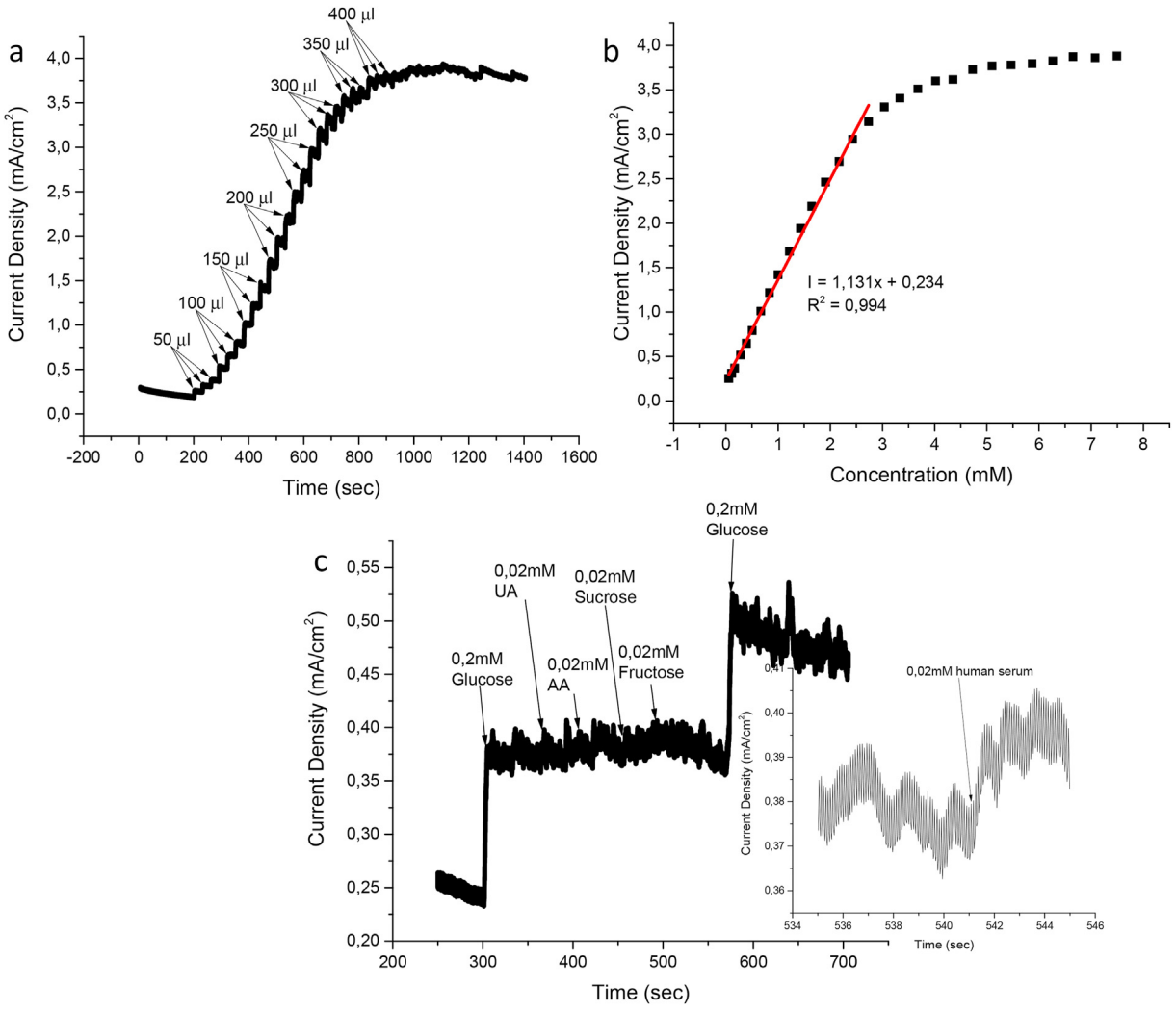

Fig. 9. Amperometric response of the N−CuO/Cu_2O:NiO sensor to a) successive additions of glucose, b) corresponding calibration curve including the linear range and c) interference species of biological samples with an inset of an 0.02 mM injection of human serum.

Table 2
Performance characteristics of the various developed sensors.

Material	Sensitivity (µA/mM.cm^2)	Linear Range (mM)	LOD (mM)
CuO	830	1.65	0.022
N−CuO/Cu_2O	873	1.91	0.014
CuO:NiO	1103	1.65	0.061
N−CuO/Cu_2O:NiO	1131	2.74	0.020

making use of the same electrode used during repeatability tests. The developed sensor exhibited an RSD of less than 3% for the repeatability (Data in Brief Figure 5b), also it has an RSD of 16% over a 4-week period. These demonstrates high repeatability and better stability of the sensor. The thin film of N−CuO/Cu_2O:NiO adheres to the FTO glass electrode after numerous CV cycles, rinsing in deionized water and dried with a compressed air blower. This excellent adhesion is shown by the minimal change of 3% in electrochemical oxidation of glucose during repeatability and 16% change for the stability tests. Also, no debris was seen floating in the electrolyte solution during the CV cycles. A comparison of the as prepared sensor performance with other nonenzymatic glucose sensors reported in the literature for glucose detection is presented Table 3. It can be seen that the electrochemical performance of the developed material is in par with the other reported sensors.

4. Conclusions

A plasma assisted nitrogen doped mixed oxide, N−CuO/Cu_2O:NiO, sensor was developed through a binder less solution-based process for biosensing applications. This study showed that plasma assisted nitrogen doping induces phase conversion of CuO to Cu_2O. The nitrogen doped mixed oxide sensor exhibited enhanced electrochemical behaviour compared to the pristine counterparts as was confirmed by cyclic voltammetry and chronoamperometry experiments. The enhanced electrochemical activity originated from the improved electronic property of the mixed oxide sensor as demonstrated by EIS, Tafel slope and hall effect measurements.

CRediT authorship contribution statement

Maghmood Palmer: Writing - original draft, preparation, Methodology, Data collection, Data curation. **Milua Masikini:** Methodology, Data collection. **Li-Wen Jiang:** Methodology, Data collection. **Jian-Jun Wang:** Methodology, Data collection. **Franscious Cummings:** Methodology, Data collection. **Jessica Chamier:** Methodology, Data collection. **Omowumi Inyang:** Methodology,

Table 3
Comparison of the N−CuO/Cu_2O:NiO sensor with previously developed sensors.

Material Used	Sensitivity (μA/mM.cm^2)	Linear Range (mM)	Reference
N−CuO/Cu_2O:NiO film	1131	0.05−2.74	this work
CuO doped NiO microfibres	3165	0.003−0.51	[15]
CuO nanowires	1800	up to 2	[19]
CuO nanofibres	431	0.006−2.5	[50]
CuO/Cu_2O nanofibres	830	up to 10	[12]
Ni doped ZrAlCo−O composite structure	1553	up to 2.8	[9]
Zn doped Co_3O_4 film	193	up to 0.62	[17]
Co_3O_4 film	398	0.021−1.74	[18]

Data collection. **Mahabubur Chowdhury:** Writing - review & editing, Supervision, Principle invetsigator.

Declaration of competing interest

The authors declare that they have no known competing financial interests or personal relationships that could have appeared to influence the work reported in this paper.

Acknowledgements

The authors would like to thank the National Research Foundation (NRF) South Africa and the Cape Peninsula university technology for financial grant (NRF Grant: 117686, and CPGS postdoctoral fellowship 2020).

References

[1] S. Carrà, Stepping Stones to Synthetic Biology, Springer, 2018.
[2] X. Xiao, S. Peng, C. Wang, D. Cheng, N. Li, Y. Dong, Q. Li, D. Wei, P. Liu, Z. Xie, Metal/metal oxide@ carbon composites derived from bimetallic Cu/Ni-based MOF and their electrocatalytic performance for glucose sensing, J. Electroanal. Chem. 841 (2019) 94−100.
[3] V. Scognamiglio, Nanotechnology in Glucose Monitoring: Advances and Challenges in the Last 10 Years, 2013.
[4] A.D. Association, Diagnosis and classification of diabetes mellitus, Diabetes Care 33 (2010) S62−S69.
[5] W. Zhang, Y. Du, M.L. Wang, Noninvasive glucose monitoring using saliva nano-biosensor, Sens. Bio-Sens. Res. 4 (2015) 23−29.
[6] Y. Du, W. Zhang, M.L. Wang, Sensing of salivary glucose using nano-structured biosensors, Biosensors 6 (2016) 10.
[7] S. Rauf, M.A. Hayat Nawaz, M. Badea, J.L. Marty, A. Hayat, Nano-engineered biomimetic optical sensors for glucose monitoring in diabetes, Sensors 16 (2016) 1931.
[8] M.A. Al-Omair, A. Touny, F.A. Al-Odail, M. Saleh, Electrocatalytic oxidation of glucose at nickel phosphate nano/micro particles modified electrode, Electrocatalysis 8 (2017) 340−350.
[9] X. Wu, F. Chen, M. Huang, Z. Dan, F. Qin, Ni-decorated ZrAlCo-O nanotube arrays with ultrahigh sensitivity for non-enzymatic glucose sensing, Electrochim. Acta 311 (2019) 201−210.
[10] Y. Guo, J. Liu, Y.-T. Xu, B. Zhao, X. Wang, X.-Z. Fu, R. Sun, C.-P. Wong, In situ redox growth of mesoporous Pd-Cu2O nanoheterostructures for improved glucose oxidation electrocatalysis, Sci. Bull. 64 (2019) 764−773.
[11] S.Y. Tee, C.P. Teng, E. Ye, Metal nanostructures for non-enzymatic glucose sensing, Mater. Sci. Eng. C 70 (2017) 1018−1030.
[12] N. Lu, C. Shao, X. Li, T. Shen, M. Zhang, F. Miao, P. Zhang, X. Zhang, K. Wang, Y. Zhang, CuO/Cu 2 O nanofibers as electrode materials for non-enzymatic glucose sensors with improved sensitivity, RSC Adv. 4 (2014) 31056−31061.
[13] S. Masudy-Panah, K. Radhakrishnan, A. Kumar, T.I. Wong, R. Yi, G.K. Dalapati, Optical bandgap widening and phase transformation of nitrogen doped cupric oxide, J. Appl. Phys. 118 (2015) 225301.
[14] Y. Ding, Y. Wang, L. Su, M. Bellagamba, H. Zhang, Y. Lei, Electrospun Co3O4 nanofibers for sensitive and selective glucose detection, Biosens. Bioelectron. 26 (2010) 542−548.
[15] F. Cao, S. Guo, H. Ma, G. Yang, S. Yang, J. Gong, Highly sensitive nonenzymatic glucose sensor based on electrospun copper oxide-doped nickel oxide composite microfibers, Talanta 86 (2011) 214−220.
[16] M. Chowdhury, C. Ossinga, F. Cummings, J. Chamier, M. Kebede, Novel Sn doped Co3O4 thin film for nonenzymatic glucose bio-sensor and fuel cell, Electroanalysis 29 (2017b) 1876−1886.
[17] M. Chowdhury, F. Cummings, M. Kebede, V. Fester, Binderless solution processed Zn doped Co3O4 film on FTO for rapid and selective non-enzymatic glucose detection, Electroanalysis 29 (2017a) 578−586.
[18] T. Gota, M. Chowdhury, T. Ojumu, Non-enzymatic fructose sensor based on Co3O4 thin film, Electroanalysis 29 (2017) 2855−2862.
[19] C. Espro, N. Donato, S. Galvagno, D. Aloisio, S.G. Leonardi, G. Neri, CuO nanowires-based electrodes for glucose sensors, Chem. Eng. 41 (2014).
[20] J. Park, K. An, Y. Hwang, J.-G. Park, H.-J. Noh, J.-Y. Kim, J.-H. Park, N.-M. Hwang, T. Hyeon, Ultra-large-scale syntheses of monodisperse nanocrystals, Nat. Mater. 3 (2004) 891.
[21] H. Song, Y. Ni, S. Kokot, A novel electrochemical sensor based on the copper-doped copper oxide nano-particles for the analysis of hydrogen peroxide, Colloid. Surface. Physicochem. Eng. Aspect. 465 (2015) 153−158.
[22] N.K. Eswar, R. Gupta, P.C. Ramamurthy, G. Madras, Influence of copper oxide grown on various conducting substrates towards improved performance for photoelectrocatalytic bacterial inactivation, Mol. Catal. 451 (2018) 161−169.
[23] D. Manyasree, K. Peddi, R. Ravikumar, CuO nanoparticles: synthesis, characterization and their bactericidal efficacy, Int. J. Appl. Pharm. 9 (2017) 71−74.
[24] L. Xu, Z. Wang, J. Wang, Z. Xiao, X. Huang, Z. Liu, S. Wang, N-doped nanoporous Co3O4 nanosheets with oxygen vacancies as oxygen evolving electrocatalysts, Nanotechnology 28 (2017) 165402.
[25] G. Muthusankar, R. Sasikumar, S.-M. Chen, G. Gopu, N. Sengottuvelan, S.-P. Rwei, Electrochemical synthesis of nitrogen-doped carbon quantum dots decorated copper oxide for the sensitive and selective detection of non-steroidal anti-inflammatory drug in berries, J. Colloid Interface Sci. 523 (2018) 191−200.
[26] X. Bai, W. Chen, Y. Song, J. Zhang, R. Ge, W. Wei, Z. Jiao, Y. Sun, Nickel-copper oxide nanowires for highly sensitive sensing of glucose, Appl. Surf. Sci. 420 (2017) 927−934.
[27] Z. Li, Y. Xin, Z. Zhang, H. Wu, P. Wang, Rational design of binder-free noble metal/metal oxide arrays with nanocauliflower structure for wide linear range nonenzymatic glucose detection, Sci. Rep. 5 (2015b) 10617.
[28] S. Cheng, S. Delacruz, C. Chen, Z. Tang, T. Shi, C. Carraro, R. Maboudian, Hierarchical Co3O4/CuO nanorod array supported on carbon cloth for highly sensitive non-enzymatic glucose biosensing, Sensor. Actuator. B Chem. 298 (2019) 126860.
[29] S. Liu, K. Hui, K. Hui, Flower-like copper cobaltite nanosheets on graphite paper as high-performance supercapacitor electrodes and enzymeless glucose sensors, ACS Appl. Mater. Interfaces 8 (2016) 3258−3267.
[30] M. Dar, Y. Kim, W. Kim, J. Sohn, H. Shin, Structural and magnetic properties of CuO nanoneedles synthesized by hydrothermal method, Appl. Surf. Sci. 254 (2008) 7477−7481.
[31] K. Dhara, T. Ramachandran, B.G. Nair, T.S. Babu, Single step synthesis of Au−CuO nanoparticles decorated reduced graphene oxide for high performance disposable nonenzymatic glucose sensor, J. Electroanal. Chem. 743 (2015) 1−9.
[32] M.C. Biesinger, Advanced analysis of copper X-ray photoelectron spectra, Surf. Interface Anal. 49 (2017) 1325−1334.
[33] M.C. Biesinger, L.W. Lau, A.R. Gerson, R.S.C. Smart, Resolving surface chemical states in XPS analysis of first row transition metals, oxides and hydroxides: Sc, Ti, V, Cu and Zn, Appl. Surf. Sci. 257 (2010) 887−898.
[34] A.J. Wagner, G.M. Wolfe, D.H. Fairbrother, Reactivity of vapor-deposited metal atoms with nitrogen-containing polymers and organic surfaces studied by in situ XPS, Appl. Surf. Sci. 219 (2003a) 317−328.
[35] M.A. Macdonald, H.A. Andreas, Method for equivalent circuit determination for electrochemical impedance spectroscopy data of protein adsorption on solid surfaces, Electrochim. Acta 129 (2014) 290−299.
[36] G. Soto, W. De La Cruz, M. Farias, XPS, AES, and EELS characterization of nitrogen-containing thin films, J. Electron. Spectrosc. Relat. Phenom. 135 (2004) 27−39.
[37] J. Zhu, H. Yin, J. Gong, M. Al-Furjan, Q. Nie, In situ growth of Ni/NiO on N-doped carbon spheres with excellent electrocatalytic performance for non-enzymatic glucose detection, J. Alloys Compd. 748 (2018) 145−153.
[38] C. Wagner, A. Naumkin, A. Kraut-Vass, J. Allison, C. Powell, J. Rumble JR, NIST X-Ray Photoelectron Spectroscopy Database, NIST Standard Reference Database 20, U. S. Department of Commerce, 2003b. Version 3.4 (Web Version).
[39] S. Kabir, K. Artyushkova, A. Serov, B. Kiefer, P. Atanassov, Binding energy shifts for nitrogen-containing graphene-based electrocatalysts−experiments and DFT calculations, Surf. Interface Anal. 48 (2016) 293−300.
[40] I. Matanovic, K. Artyushkova, M.B. Strand, M.J. Dzara, S. Pylypenko, P. Atanassov, Core level shifts of hydrogenated pyridinic and pyrrolic nitrogen in the nitrogen-containing graphene-based electrocatalysts: in-plane vs edge

defects, J. Phys. Chem. C 120 (2016) 29225–29232.
[41] S. Zheng, B. Li, Y. Tang, Q. Li, H. Xue, H. Pang, Ultrathin nanosheet-assembled [Ni 3 (OH) 2 (PTA) 2 (H 2 O) 4]· 2H 2 O hierarchical flowers for high-performance electrocatalysis of glucose oxidation reactions, Nanoscale 10 (2018) 13270–13276.
[42] V.M. Donnelly, A. Kornblit, Plasma etching: yesterday, today, and tomorrow, J. Vac. Sci. Technol.: Vacuum, Surfaces, and Films 31 (2013), 050825.
[43] F. Werner, Hall measurements on low-mobility thin films, J. Appl. Phys. 122 (2017) 135306.
[44] T. Gessert, J. Burst, X. Li, M. Scott, T. Coutts, Advantages of transparent conducting oxide thin films with controlled permittivity for thin film photovoltaic solar cells, Thin Solid Films 519 (2011) 7146–7148.
[45] M. Tyagi, M. Tomar, V. Gupta, Influence of hole mobility on the response characteristics of p-type nickel oxide thin film based glucose biosensor, Anal. Chim. Acta 726 (2012) 93–101.
[46] Y. Zhang, Y. Liu, L. Su, Z. Zhang, D. Huo, C. Hou, Y. Lei, CuO nanowires based sensitive and selective non-enzymatic glucose detection, Sensor. Actuator. B Chem. 191 (2014) 86–93.
[47] C. Zhao, C. Shao, M. Li, K. Jiao, Flow-injection analysis of glucose without enzyme based on electrocatalytic oxidation of glucose at a nickel electrode, Talanta 71 (2007) 1769–1773.
[48] D. Iwueke, C. Amaechi, A. Nwanya, A. Ekwealor, P. Asogwa, R. Osuji, M. Maaza, F. Ezema, A novel chemical preparation of Ni (OH) 2/CuO nanocomposite thin films for supercapacitive applications, J. Mater. Sci. Mater. Electron. 26 (2015) 2236–2242.
[49] L.-Y. Lin, B.B. Karakocak, S. Kavadiya, T. Soundappan, P. Biswas, A highly sensitive non-enzymatic glucose sensor based on Cu/Cu2O/CuO ternary composite hollow spheres prepared in a furnace aerosol reactor, Sensor. Actuator. B Chem. 259 (2018) 745–752.
[50] W. Yi, J. Liu, H. Chen, Y. Gao, H. Li, Copper/nickel nanoparticle decorated carbon nanotubes for nonenzymatic glucose biosensor, J. Solid State Electrochem. 19 (2015) 1511–1521.
[51] J. Yang, W. Tan, C. Chen, Y. Tao, Y. Qin, Y. Kong, Nonenzymatic glucose sensing by CuO nanoparticles decorated nitrogen-doped graphene aerogel, Mater. Sci. Eng. C 78 (2017a) 210–217.
[52] S. Yang, G. Li, D. Wang, Z. Qiao, L. Qu, Synthesis of nanoneedle-like copper oxide on N-doped reduced graphene oxide: a three-dimensional hybrid for nonenzymatic glucose sensor, Sensor. Actuator. B Chem. 238 (2017b) 588–595.
[53] N. Gowthaman, M.A. Raj, S.A. John, Nitrogen-doped graphene as a robust scaffold for the homogeneous deposition of copper nanostructures: a nonenzymatic disposable glucose sensor, ACS Sustain. Chem. Eng. 5 (2017) 1648–1658.
[54] Y. Ding, Y. Wang, L. Su, M. Bellagamba, H. Zhang, Y. Lei, Electrospun Co3O4 nanofibers for sensitive and selective glucose detection, Biosens. Bioelectron. 26 (2010) 542–548.
[55] R.S. Nicholson, I. Shain, Theory of stationary electrode polarography. Single scan and cyclic methods applied to reversible, irreversible, and kinetic systems, Anal. Chem. 36 (1964) 706–723.
[56] A. Electrochemistry, in: J. Wang (Ed.), Wiley VCH, New York, 2000.
[57] G. Karim-Nezhad, R. Jafarloo, P.S. Dorraji, Copper (hydr) oxide modified copper electrode for electrocatalytic oxidation of hydrazine in alkaline media, Electrochim. Acta 54 (2009) 5721–5726.
[58] X. Li, D. Luo, X. Zhang, Z. Zhang, Enhancement of electrochemical performances for LiFePO4/C with 3D-grape-bunch structure and selection of suitable equivalent circuit for fitting EIS results, J. Power Sources 291 (2015a) 75–84.
[59] F. Fasmin, R. Srinivasan, Nonlinear electrochemical impedance spectroscopy, J. Electrochem. Soc. 164 (2017) H443–H455.
[60] W. Choi, H.-C. Shin, J.M. Kim, J.-Y. Choi, W.-S. Yoon, Modeling and applications of electrochemical impedance spectroscopy (EIS) for lithium-ion batteries, J. Electrochem. Sci. Technol. 11 (2020) 1–13.
[61] G. Reach, G.S. Wilson, Can continuous glucose monitoring be used for the treatment of diabetes, Anal. Chem. 64 (1992) 381A–386A.
[62] C.-Y. Ko, J.-H. Huang, S. Raina, W.P. Kang, A high performance non-enzymatic glucose sensor based on nickel hydroxide modified nitrogen-incorporated nanodiamonds, Analyst 138 (2013) 3201–3208.